J. Opt. A: Pure Appl. Opt. **2** (2000) 314–318. Printed in the UK PII: S1464-4258(00)10387-3

Measurement of nonlinear polarization rotation in a highly birefringent optical fibre using a Faraday mirror

C Vinegoni, M Wegmuller, B Huttner and N Gisin

Group of Applied Physics, University of Geneva, 20 Ecole-de-Medecine, CH-1211 Geneve 4, Switzerland

E-mail: claudio.vinegoni@physics.unige.ch

Received 14 December 1999, in final form 30 March 2000

Abstract. We present both a theoretical and experimental analysis of nonlinear polarization rotation in an optical fibre. Starting from the coupled nonlinear Schrödinger equations an analytical solution for the evolution of the state of polarization, valid for fibres with large linear birefringence and quasi cw input light with arbitrary polarization, is given. It allows us to model straightforwardly go-and-return paths as in interferometers with standard or Faraday mirrors. In the experiment all the fluctuations in the linear birefringence, including temperature- and pressure-induced ones, are successfully removed in a passive way by using a double pass of the fibre under test with a Faraday mirror at the end of the fibre. This allows us to use long fibres and relatively low input powers. The match between the experimental data and our model is excellent, except at higher intensities where deviations due to modulation instability start to appear.

Keywords: Nonlinear polarization rotation, nonlinear birefringence, Keff effect, Faraday mirror

1. Introduction

The potential of nonlinear polarization rotation (NPR) to build ultrafast devices was recognized a long time ago and has received considerable attention since then. It has been proposed to exploit it for optical switches [1], logic gates [2], multiplexers [3], intensity discriminators [4], nonlinear filters [5], or pulse shapers [6]. However, an inherent problem with all these applications is the stability of the output state of polarization, generally subjected to fluctuations of the linear birefringence caused by temperature changes and drafts in the fibre environment. Of course, the same problem was also encountered in the few experiments dealing with the characterization and measurement of the NPR itself. In [7], the fluctuations of the output polarization were too strong to allow a meaningful measurement of NPR in a polarization maintaining fibre at 1064 nm, and in [8], where 514 nm light was injected into a 60 m long fibre with a beat length of 1.6 cm, a complicated arrangement had to be employed for the extraction of the changes caused by temperature drifts.

As the fluctuations become worse for fibres with a large birefringence, and as the effect of NPR is proportional to the inverse of the wavelength, it is hard to measure NPR directly in a polarization-maintaining (PM) fibre at the telecom wavelength of 1.55 μm. In this work we propose a method for removing the overall linear birefringence, and therefore also its fluctuations, in a passive way by employing a Farady mirror (FM) [9] and a double pass of the fibre under test. To check how this—nowadays standard—method [10–13] of removing linear birefringence acts on the NPR, we develop in section 2 of this paper a simple model to calculate the action of linear and nonlinear birefringence. Using this model, it is then easy to show that the proposed method removes the overall linear birefringence only, whereas the nonlinear one, leading to NPR, remains unchanged. After describing the experimental setup, the results of our NPR measurements using a FM are presented in section 3, along with the predictions from our analytical model. The excellent agreement between the two demonstrates that using the FM, the overall linear birefringence is indeed removed completely, allowing one to observe the NPR otherwise hidden within the noisy background of polarization changes due to environmental perturbations. This result also validates our method for possible implementation with a variety of other applications like the ones mentioned at the beginning of this section, with the prospect of drastically increasing their polarization stability.

2. Theoretical background

In a dielectric medium, an intense elliptical input pulse induces birefringence—via the optical Kerr effect—due to

1464-4258/00/040314+05$30.00

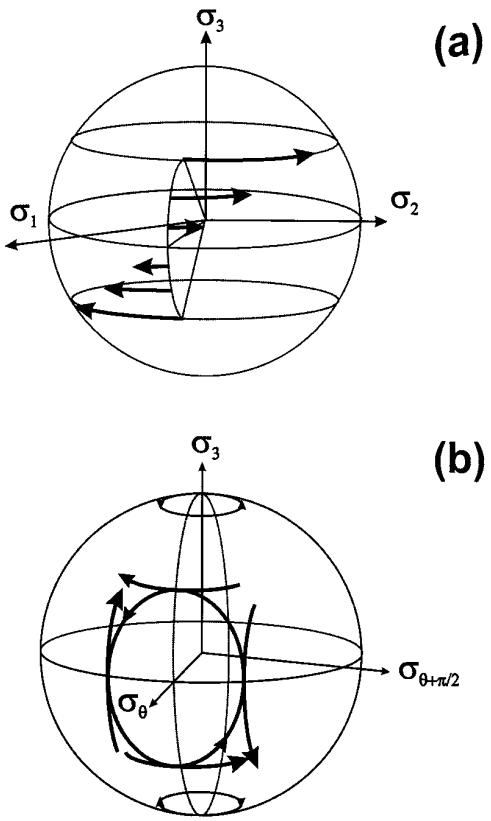

Figure 1. Evolution of the state of polarization as represented on the Poincaré sphere. (*a*) Polarization ellipse self-rotation in an isotropic medium. The Stokes vector is rotating around the σ_3 axis with an angle proportional to the length of the medium, the input intensity, and the sine of the input ellipticity.
(*b*) High-birefringence fibre. The rotation of the Stokes vector mainly consists of a fast rotation around the axis of linear birefringence σ_θ, whereas the slow rotations due to the nonlinear birefringence can be considered as small perturbations.

the different amounts of intensity along the major and minor axis of the polarization ellipse. It is well known that in isotropic media this self-induced birefringence leads to a rotation of the polarization ellipse while propagating in the medium [14, 15] (the effect is consequently often called polarization ellipse self-rotation and its representation on the Poincaré sphere is shown in figure 1(*a*)). In fact, measuring this ellipse rotation is one of the standard ways to evaluate the cubic optic nonlinearity of the medium [16]. In an optical fibre however, the situation becomes more complicated as there is also the local intrinsic birefringence to be considered. Generally, the polarization ellipse changes are hard to predict in that case as the linear and nonlinear birefringence interact in a complicated manner.

To formulate this more precisely, we start with the coupled nonlinear Schrödinger equations describing the propagation of light in an optical fibre. For cw input light, time derivatives drop out, and we can write the equation in a similar form as Menyuk [17] when assuming a lossless, linearly birefringent fibre and by neglecting polarization mode coupling:

$$\partial_z \psi = -\mathrm{i}(\omega B \sigma_\theta + \omega\alpha \langle\sigma_3\rangle_\psi \sigma_3)\psi. \tag{1}$$

$\psi = (E_1, E_2)^t$ is the Jones column vector representing the two components of the complex transverse electric fields $E_1(z)$ and $E_2(z)$ at the position z along the fibre. The first term in the right-hand side describes the linear birefringence, where ω is the optical frequency and B the birefringence (in s m^{-1}). Note that B is assumed to be independent of ω, an excellent approximation for standard fibres. The phase birefringence ωB is multiplied by $\sigma_\theta = \sigma_1 \cos(\theta) + \sigma_2 \sin(\theta)$, corresponding to linear birefringence in the θ direction, with $\sigma_{1,2,3}$ being the 2×2 Pauli matrices. The second term in the right-hand side of (1) accounts for the nonlinear birefringence, with $\alpha = \frac{n_2 P}{3cA_{\mathrm{eff}}}$, and $\langle\sigma_3\rangle_{\psi_z} = \frac{|E_1|^2 - |E_2|^2}{|E_1|^2 + |E_2|^2}$. P is the total light power, n_2 the nonlinear refractive index, A_{eff} the effective mode area, and c the speed of light.

For an intuitive understanding of the action of the two terms in the right-hand side of (1), it is better to revert to the Stokes formalism. On the Poincaré sphere, the first term describes a rotation of the polarization vector (Stokes vector) around axis σ_θ, lying on the equator and corresponding to linear birefringence. Similarly, the second term is a rotation around the vertical axis corresponding to nonlinear birefringence. However, equation (1) shows that the speed and the rotation direction in this case depends on the polarization state through $\langle\sigma_3\rangle_\psi$, as is illustrated in figure 1(*b*). Consequently, the two rotations are linked in a complicated manner, and the resulting evolution of the polarization vector is not obvious.

Fortunately, in standard telecom fibres, the speed of rotation around the vertical axis is much smaller than the one around the birefringent axis σ_θ even at considerable power levels. This is because in such fibres $B \gg \alpha$ (see (1)). For example, a fibre with a beat length of 10 m has $B \approx 0.5$ ps km^{-1} while $\alpha \approx 0.006$ ps km^{-1} for a power of 10 W ($\lambda = 1550$ nm, $n_2 = 3.2 \times 10^{-20}$, $A_{\mathrm{eff}} = 60\ \mu\mathrm{m}^2$) (note that in this work, a PM fibre will be used with a beat length in the mm range, making the ratio $\frac{B}{\alpha}$ as large as 10^7). The slow rotation due to the nonlinear birefringence can therefore be treated as a perturbation that merely changes the angular frequency of the fast rotation caused by the linear birefringence. This becomes more obvious by rewriting (1) as

$$\begin{aligned}\partial_z \psi = & -\mathrm{i}\omega B \sigma_\theta \psi - \mathrm{i}\omega\alpha \tfrac{1}{2}(\langle\sigma_3\rangle_\psi \sigma_3 \\ & + (1 - \langle\sigma_{\theta+\frac{\pi}{2}}\rangle_\psi \sigma_{\theta+\frac{\pi}{2}} - \langle\sigma_\theta\rangle_\psi \sigma_\theta))\psi\end{aligned} \tag{2}$$

where the identity $\psi = \langle\sigma\rangle_\psi \sigma\psi$, valid for all ψ, has been used. The term proportional to ψ affects only the global phase and can be neglected. Further, the two terms $\langle\sigma_3\rangle_\psi \sigma_3$ and $\langle\sigma_{\theta+\frac{\pi}{2}}\rangle_\psi \sigma_{\theta+\frac{\pi}{2}}$ cancel each other to first order—this can be intuitively understood from figure 1(*b*) and was confirmed by numerical simulations—producing only a small (second-order) precession of the instantaneous rotation axis. Hence we obtain the following approximation for the evolution of the polarization vector:

$$\partial_z \psi \approx -\mathrm{i}\omega B_{\mathrm{eff}} \sigma_\theta \psi \tag{3}$$

with the effective birefringence

$$B_{\mathrm{eff}} = B - \frac{\alpha}{2}\langle\sigma_\theta\rangle_\psi \tag{4}$$

depending on the intensity and the polarization state of the input light signal. Note that equation (3) preserves the square norm $|\psi|^2$ reflecting that we did not take into account losses. Note further that when applying (3) for linearly polarized input light we obtain the same formula as in [4].

The solution of (3) is straightforward, $\psi_z = \exp(-\mathrm{i}\omega B_{\mathrm{eff}}\sigma_\theta z)\psi_0$, and corresponds to a rotation of the input polarization vector around the linear birefringence axis σ_θ, with a rotation angle β given by

$$\beta = \omega\left(B - \frac{\alpha}{2}m_\theta(0)\right)z. \tag{5}$$

$m_\theta(0)$ is the projection of the input polarization vector on the birefringence axis σ_θ, and z the distance from the input end.

In principle, the NPR, caused by the nonlinear response of the single-mode fibre to the input state, could now be measured by varying the input power and observing the corresponding change in the output polarization vector. However, from a practical standpoint, this will be hardly possible as equation (5) shows that slightest changes in the linear birefringence B will completely cover the nonlinear, intensity-dependent ones (remember that $B \gg \alpha$ for reasonable input power levels). Indeed, earlier work [8, 18] greatly suffered from temperature- and pressure-induced changes of B always present in a laboratory environment, even though they were using short fibres.

Nowadays, a simple and efficient way to get rid of any kind of fluctuation in the intrinsic birefringence is to make a double pass of the fibre under test by means of a FM [9, 10]. The linear birefringence accumulated during the forward path is then automatically compensated on the return path. However, it is not *a priori* clear what will happen to the nonlinear birefringence.

To investigate this point, we rewrite the solution of (3) in the Stokes formalism,

$$\boldsymbol{m}(L) = \hat{\boldsymbol{R}}_\theta(\beta(L))\boldsymbol{m}(0) \tag{6}$$

where $\boldsymbol{m}(0)$ is the input Stokes vector, $\hat{\boldsymbol{R}}_\theta$ is a rotation operator around the axis σ_θ, and β is as given by (5). Applying the action of the FM, $\boldsymbol{m}^F(L) = -\boldsymbol{m}(L)$ (the superscript F indicates the state of polarization after reflection from the FM), and of the return path, $\hat{\boldsymbol{R}}_\theta^{-1}$, we get

$$\begin{aligned}\boldsymbol{m}^F(2L) &= \hat{\boldsymbol{R}}_\theta^{-1}\left[\omega L\left(B - \frac{\alpha}{2}m_\theta^F(L)\right)\right]\hat{\boldsymbol{R}}_\theta \\ &\quad\times\left[\omega L\left(B - \frac{\alpha}{2}m_\theta(0)\right)\right]\boldsymbol{m}(0) \\ &= -\hat{\boldsymbol{R}}_\theta[\omega\alpha L m_\theta(0)]\boldsymbol{m}(0).\end{aligned} \tag{7}$$

The result shows that the rotation due to the nonlinear birefringence of the forward and return path do not cancel out but add, giving twice the angle compared with a single (forward) trip through the fibre (equation (5)). This is because the rotation direction of the nonlinear birefringence is different for the upper and lower hemisphere of the Poincaré sphere (see figure 1(*b*)) contrary to birefringence in linear optics. Therefore, after reflection at the FM, which transforms the polarization state to its orthogonal counterpart (i.e. flipping it to the other hemisphere), the sense of rotation of the NPR during the return path will be the same as the forward path and the effects add up.

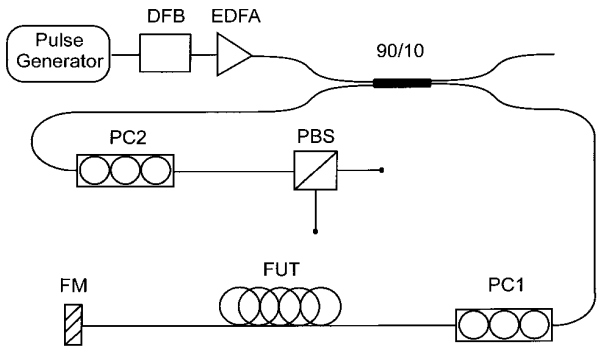

Figure 2. Experimental setup of the NPR measurement. DFB, distributed feedback laser; EDFA, erbium-doped fibre amplifier; PC, polarization controller; FUT, fibre under test; FM, Faraday mirror; PBS, polarizing beam splitter.

3. Experiment

3.1. Setup

The experimental setup used to measure the NPR is shown in figure 2. The light source is a distributed feedback laser diode (DFB) operated in pulsed mode at a wavelength of 1559 nm, consecutively amplified by an EDFA (small signal gain 40 dB, saturated output power 23 dBm, where dBm is a physical unit of power). Typically, pulses with a duration of 30 ns, a repetition rate of 1 kHz and a peak power of up to 6 W were used. The light is then launched into the test fibre via a 90/10 coupler and a polarization controller. The coupler was inserted for the detection of the backward-travelling light after the double pass of the test fibre, with its 90-output port connected to the source in order to maintain the high launch powers into the test fibre. The polarization controller, PC1, allowed us to adjust the polarization of the light launched into the test fibre, which is important for the strength of the NPR as demonstrated by equation (5).

In order to satisfy the assumption of neglectable polarization mode coupling used in the previous section, a highly birefringent, PM fibre was used as the test fibre. Its linear birefringence B is of the order of 5 ps m^{-1}, corresponding to a beat length in the mm range. The fibre length was 200 m, giving a total of 400 m round-trip length of the light reflected by the FM.

The polarization state of the light after the double pass of the test fibre was examined by an analyser consisting of a polarization controller PC2 and a polarizing beam splitter (PBS). To achieve a good sensitivity of the analyser, it was calibrated to give a 50/50 output of the PBS for low-power signals where no nonlinear polarization rotation occurs. Finally, the two PBS output channels were monitored by a fast photodiode (200 ps response time) and a sampling scope.

The measurements were then performed in the following way: for a given launch power, the polarization controller PC1 was adjusted to give the smallest possible output power at the monitored PBS channel. Consequently, the difference between the two PBS output channels is maximized, corresponding to a maximum value of the NPR.

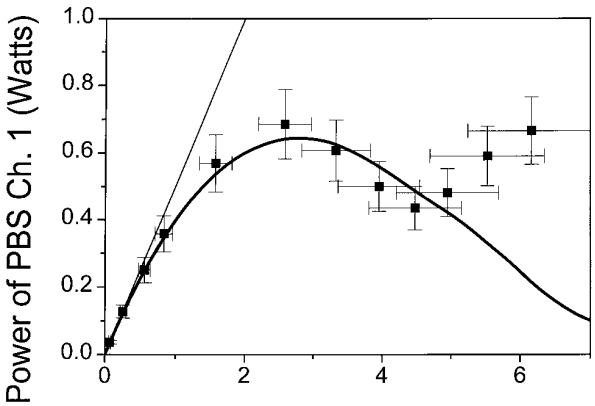

Figure 3. Minimum output power of PBS channel 1 as a function of the launched power for a 200 m long PM fibre. Squares: measured data; solid curve: prediction from our model; straight line: prediction in the absence of NPR. The deviations of the experimental data from the predicted values at high powers are due to modulation instability not included in the model.

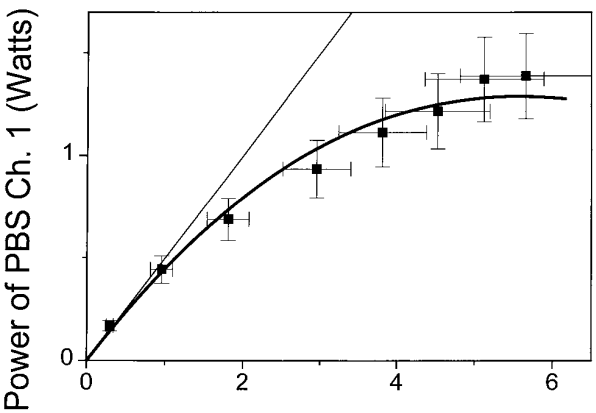

Figure 4. Minimum output power of PBS channel 1 as a function of the launched power for a 100 m long PM fibre. Squares: measured data; solid curve: prediction from our model; straight line: prediction in the absence of NPR.

3.2. Results

The experimental results are shown in figures 3 and 4.

In figure 3, the minimum output power (squares) of the monitored PBS channel is given as a function of the peak power in the test fibre. Note that the reported output power was normalized to account for the analyser losses and corrected for the PBS extinction ratio. Consequently, without any NPR, the reported output power would equal half of the power in the test fibre (straight line). As can be seen in figure 3, the effect of NPR is negligibly small up to about 0.5 W. For higher launch powers, NPR manifests itself by a reduction of the power in the monitored PBS channel. In fact, its action becomes so strong that for launch powers above about 2.5 W, the output power starts actually to decrease in spite of the linear increase that would be experienced in the absence of NPR. In principle, this power drop should continue until the nonlinear rotation of the input polarization is such that all the power is in the other PBS channel. However, as figure 3 shows, this is not happening. The observed increase in the minimum output power could be related to modulation instability: above 4.5 W launch power, a Stokes and anti-Stokes sideband shifted by 2 nm with respect to the laser peak appeared. These sidebands are generated in a distributed fashion along the test fibre, which means that the compensation of the linear fibre birefringence is failing. Therefore, and due to the large birefringence B of the PM fibre used, the sidebands will be almost randomly polarized at the output. As a consequence, about half of the power transferred to the sidebands will appear in the monitored PBS output channel leading to the observed increase in power.

Further, the measured results were compared with the ones predicted by equation (8), taking into account the analyser calibration and the adjustment of PC1 as used in the experiment. The parameters used in the computation were the ones from the experiment, i.e. a fibre length of $L = 200$ m, and a nonlinear coefficient of $n_2 = 3.4 \times 10^{-20}$ m^2 W^{-1}. The effective core area of $A_{\text{eff}} = 41$ μm^2 was chosen to give a good match with the experimental results as we had no exact value from the manufacturer. $m_\theta(0)$, the projection of the input state of polarization on the birefringent axis, was varied in order to give a minimum output power from the PBS channel, exactly like in the experiment.

The solid curve in figure 3 shows these computed results. The figure clearly illustrates that the measured data correspond very well with the computed results. This validates our measurement method of NPR in optical fibres and demonstrates that the linear birefringence and its detrimental fluctuations are successfully removed by the FM. Above an input power of 4.5 W, the curves deviate as expected from the onset of MI that was not included in the analytical model.

Figure 4 shows experimental and computed results for a fibre length of 100 m. Note that to avoid cutting our 200 m piece, we emulated the 100 m fibre length by introducing a 20 dB attenuation for the reflected light. Consequently, the light power on the return trip is too low to induce NPR, and serves only to compensate for the linear birefringence of the forward trip. As the figure demonstrates, NPR is indeed reduced by a factor of two compared with the measurements without attenuator, as expected from equation (8). Twice the launch power is required to compensate for the shortened length to get the same amount of NPR. Again, experimental and computed data are in excellent agreement.

The experimental results of this section clearly demonstrate that one can indeed use a FM to remove the overall linear birefringence, which allows one to observe the smallest nonlinear effects otherwise hidden within the noisy linear birefringence. Note that the change in the output polarization due to environmental perturbations is especially pronounced in PM fibres (when the input is not aligned with one of the two fibre axes) due to its short beat length in the mm range. When not using a FM, the output polarization changed (for example) drastically when just approaching the fibre spool with the hands, inhibiting any meaningful measurement.

4. Conclusion

Starting from the nonlinear Schrödinger equations, an analytical solution for the evolution of the state of polarization in a high-birefringence optical fibre has been developed. It

allows for a simple and straightforward modelling of go and return paths as, for example, in interferometers with standard or Faraday mirrors. Using this model, we showed that it is possible to remove the overall linear birefringence in a double-pass arrangement with a FM while at the same time leaving the nonlinear birefringence, resulting in NPR, unchanged. Only this arrangement allowed us to measure the NPR in a long PM fibre at telecom wavelength in a laboratory environment where it is otherwise hidden by the changes in the output polarization caused by temperature and pressure fluctuations.

The experimental results for the NPR obtained with a 200 m long PM fibre at a wavelength of 1.55 μm were in excellent agreement with the theoretical predictions from our model for launch power up to 4.5 W. Above that value deviations due to modulation instability, not included in our model, were present. Further work to apply our model to standard, non-PM fibres where the coupling between the polarization modes is not negligible, is in progress.

Due to its generality, the presented method of removing the linear birefringence while leaving the nonlinear one unchanged might prove to be a very valuable tool in numerous other applications as well, such as, for example, optical multi-/demultiplexers.

Note that in the case of non-PM fibres, where the coupling between the polarization modes is not negligible, NPR is reduced due to a scrambling related to the ratio between the coupling length and the fibre length. In fact, this effect can be exploited to get information about the important coupling length parameter in standard fibres, as will be shown elsewhere.

Acknowledgments

We acknowledge the financial support from the Swiss Federal Office for Education and Sciences (OFES) in the framework of the European COST P2 action. Further, we would like to thank the Laboratoire de Metrologie des Fibres Optique, EPFL Lausanne, for the loan of the PM fibre, and C R Menyuk for stimulating discussion on the subject.

References

[1] Olssono B E and Andrekson P A 1998 Polarization independent Kerr-switch using a polarization diversity loop *ECOC'98 (Madrid, Spain) Technical Digest* pp 185–6

[2] Kitayama K, Kimura Y and Seikai S 1985 Fibre-optic logic gate *Appl. Phys. Lett.* **46** 317–19

[3] Morioka T, Saruwatari M and Takada A 1987 Ultrafast optical multi/demultiplexer utilizing optical Kerr effect in polarization-maintaining single-mode fibres *Electron. Lett.* **23** 453–4

[4] Stolen R H, Botineau J and Ashkin A 1982 Intensity discrimination of optical pulses with birefringent fibres *Opt. Lett.* **7** 512–14

[5] Horowitz M and Silberberg Y 1997 Nonlinear filtering by use of intensity-dependent polarization rotation in birefringent fibres *Opt. Lett.* **22** 1760–2

[6] Hofer M, Fermann M E, Haberl F, Ober M H and Schmidt A J 1991 Mode locking with cross-phase and self-phase modulation *Opt. Lett.* **16** 502–4

[7] Dianov E M, Zakhidov E A, Karasik A Ya, Kasymdzhanov M A and Mirtadzhiev F M 1987 Optical Kerr effect in glass fibre waveguides with weak and strong birefringence *Sov. J. Quantum Electron.* **17** 517–19

[8] Crosignani B, Piazzola S, Spano P and Di Porto P 1985 Direct measurement of the nonlinear phase shift between the orthogonally polarized states of a single-mode fibre *Opt. Lett.* **10** 89–91

[9] Martinelli M 1989 A universal compensator for polarization changes induced by birefringence on a retracing beam *Opt. Commun.* **72** 341–4

[10] Ribordy G, Gautier J D, Gisin N, Guinnard O and Zbinden H 1998 Automated plug and play quantum key distribution *Electron. Lett.* **34** 2116–17

[11] Breguet J, Pellaux J P and Gisin N 1995 Photoacoustic detection of trace gases with an optical microphone *Sensors Actuators* A **1** 29–35

[12] Yamashita S, Hotate K and Ito M 1996 Polarization properties of a reflective fibre amplifier employing a circulator and a Faraday rotator mirror *J. Lightwave Technol.* **14** 385–90

[13] Alekseev E I, Bazarov E N, Gubin V P, Sazonov A I and Starostin N I 1999 Compensation for spurious polarization modulation in a fibre optic phase modulator with the Faraday mirror *Radiotekh. Elektron.* **44** 122–7

[14] Maker P D, Terhune R W and Savage C M 1964 Intensity-dependent changes in the refractive index of liquids *Phys. Rev. Lett.* **12** 507–9

[15] Unsbo P and Flytzanis C 1997 Degenerate four-wave mixing in isotropic nonlinear-optical gyrotropic media *J. Opt. Soc. Am.* B **14** 560–69

[16] Svirko Yu P and Zheludev N I 1998 *Polarization of Light in Nonlinear Optics* (New York: Wiley)

[17] Menyuk C R 1987 Nonlinear pulse propagation in birefringence optical fibres *IEEE J. Quantum Electron.* **23** 174–6
see also Menyuk C R 1989 Pulse propagation in an elliptically birefringent Kerr medium *IEEE J. Quantum Electron.* **25** 2674–82

[18] Dziedzic J M, Stolen R H and Aschkin A 1981 Optical Kerr effect in long fibres *Appl. Opt.* **20** 1403–6